LAWRENCE
LIVERMORE
NATIONAL
LABORATORY

LLNL-JRNL-820214

The Underlying Simplicity of 5f Unoccupied Electronic Structure

J. G. Tobin, S. Nowak, S. W. Yu, P. Roussel, R. Alonso-Mori, T. Kroll, D. Nordlund, T. C. Weng, D. Sokaras

March 5, 2021

Journal of Vacuum Science & Technology A

Disclaimer

The Underlying Simplicity of 5f Unoccupied Electronic Structure

J. G. Tobin,[1],* S. Nowak,[2] S.-W. Yu[3], P. Roussel[4], R. Alonso-Mori,[2] T. Kroll,[2]

D. Nordlund,[2] T.-C. Weng,[2] and D. Sokaras[2],*

[1]University of Wisconsin-Oshkosh, Oshkosh, WI, USA 54901, USA

[2]SLAC National Accelerator Laboratory, Menlo Park, CA 94025, USA

[3]Lawrence Livermore National Laboratory, Livermore, CA, 94550, USA

[4]AWE plc, Aldermaston, Reading, Berkshire, RG7 4PR, UK

*Contact Authors Email: tobinj@uwosh.edu and dsokaras@slac.stanford.edu

Abstract

Using a simple empirical model based upon the Bremstrahlung Isochromat Spectroscopy (BIS) of elemental Th, it is possible to explain the recent High Energy Resolution Fluorescence Detection (HERFD) measurements of UF_4 (n =2) and UCd_{11} (n =3) as well as the new Inverse Photoelectron Spectroscopy (IPES) of Pu_2O_3 (n=5), where n is the 5f occupation number. A critical issue in this analysis is the assumption that the Th 5f states are essentially empty, which will be confirmed both experimentally and computationally. Thus, for 5f localized systems, this simple model provides a unified and consistent picture of 5f Unoccupied Density of States (UDOS) in simple, localized systems, as the 5f occupation varies in the early part of the series.

The Underlying Simplicity of 5f Unoccupied Electronic Structure

I INTRODUCTION

While viewed with concern, trepidation, dislike and even hatred, Actinides are an important part of a modern technological society. [1,2] In a world fixated upon the dangers of over-reliance upon fossil fuels, nuclear power may provide a pathway to lowering the carbon footprint of energy production. [2] Historically, there are many countries with a substantial fraction of their electrical power grid supplied by nuclear power: e.g, the United States (~20%), France (~70) and Sweden (~34%), to name just a few. [3] However, nuclear power does not come without its own issues, amongst them waste disposal [4], safety [2] and non-proliferation. [1] Thus, a scientific understanding of the actinides is an important goal.

Despite the importance of this understanding, a thorough comprehension of 5f electronic structure remains elusive. In the fairly recent past, a significant development was the demonstration that Russel-Saunders Coupling Model fails in the Pu 5f states [5] and that the 5f Total Angular Momentum Coupling in the early actinides was best described by a jj-skewed Intermediate Coupling Model [6,7]. While these spectroscopic observations were explained with a Total Angular Momentum picture founded upon Cowan's code [8], the connection to the 5f Density of States (DOS) as a function of energy remained muddled. Kutepov's calculation [7] of the Occupied DOS (ODOS) and Unoccupied DOS (ODOS) of elemental U and elemental Th matched very nicely [9-11] with the corresponding X-ray Photoelectron Spectroscopy (XPS) and Bremstrahlung Isochromat Spectroscopy (BIS) of metallic U and Th of Baer and Lang [12,13], but a broader understanding was missing.

The Underlying Simplicity of 5f Unoccupied Electronic Structure

Here, the development and application of a simple model is described, which can explain the 5f UDOS behavior in uncomplicated, localized systems over the entire range of the early actinides. As shown in Figures 1, 2 and 3, this simple model can reproduce the essence of the spectral observations for UF_4 (n = 2) [14], UCd_{11} (n = 3) [14] and Pu_2O_3 (n = 5) [15], where n is the 5f occupation This includes the separate measurement of the $5f_{5/2}$ UDOS and $5f_{7/2}$ UDOS with High Energy Resolution Fluorescence Detection (HERFD) in X-ray Absorption Spectroscopy (XAS) [14,16], as well as the total UDOS from the Inverse Photoelectron Spectroscopy (IPES) of Plutonium Sesquioxide, Pu_2O_3.[15]

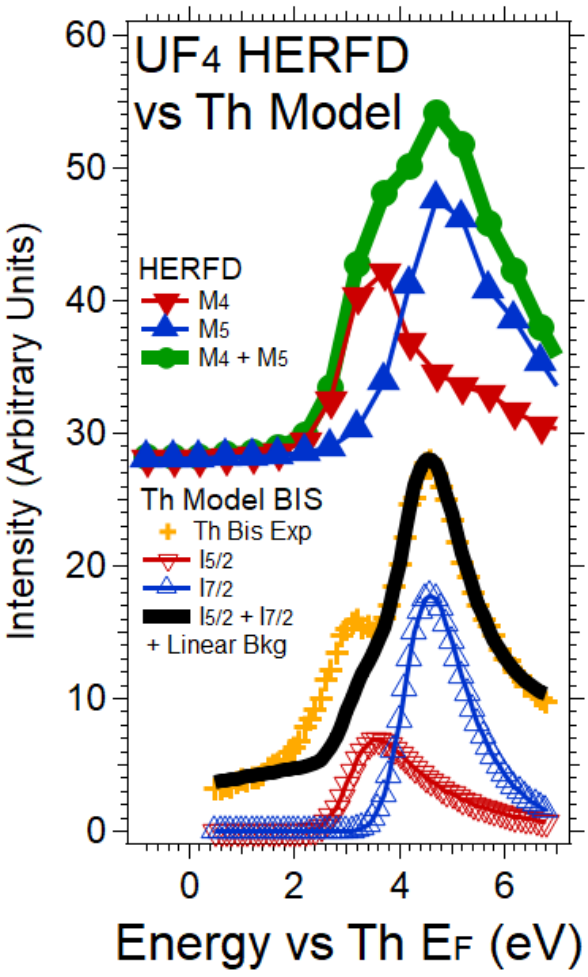

Figure 1 Shown here is a comparison between the HERFD XAS results for uranium tetrafluoride and the prediction of the Th Model for localized n = 2. (Compare red to red, blue to blue and black to green.) For the HERFD: The $M_{4,5}$ HERFD was horizontally aligned with EXAFS, a shift of 176 eV, and vertically scaled with EXAFS and the BR peak intensities (BR = 0.68 and I_{M4}: I_{M5} = 0.47). [14] The HERFD was then shifted together horizontally to align with the Th BIS energy scale and vertically to facilitate comparison. Th Model: for the n = 2 localized case, 2 electrons were added to the $5f_{5/2}$ manifold and no electrons were added to the $5f_{7/2}$ manifold, leaving a 5/2 hole to 7/2 hole ratio of 0.5. This was done using a gaussian step cutoff with a FWHM of 1.0 eV, positioned horizontally targeting a 5/2 hole to 7/2 hole ratio of ½ at an Energy of 7.0 eV.

The Underlying Simplicity of 5f Unoccupied Electronic Structure

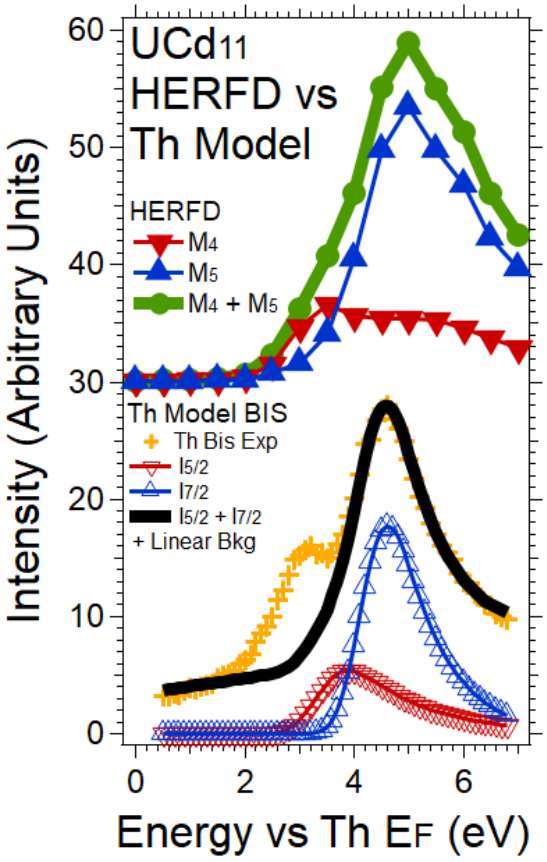

Figure 2 *Presented here is a comparison between the HERFD XAS results for uranium cadmium and the prediction of the Th Model for localized n = 3. (Compare red to red, blue to blue and black to green.) For the HERFD: The $M_{4,5}$ HERFD was horizontally aligned with EXAFS, a shift of 176 eV, and vertically scaled with EXAFS and the BR peak intensities (BR = 0.723 and I_{M4}: I_{M5} = 0.38). [14] The HERFD was then shifted together horizontally to align with the Th BIS energy scale and vertically to facilitate comparison. Th Model: for the n = 3 localized case, 2.8 electrons were added to the $5f_{5/2}$ manifold and 0.2 electrons were added to the $5f_{7/2}$ manifold, aiming for a 5/2 hole to 7/2 hole ratio of 0.41. This was done using a gaussian step cutoff with a FWHM of 1.0 eV, positioned horizontally producing a 5/2 hole to 7/2 hole ratio of 0.4 at an Energy of 7.0 eV.*

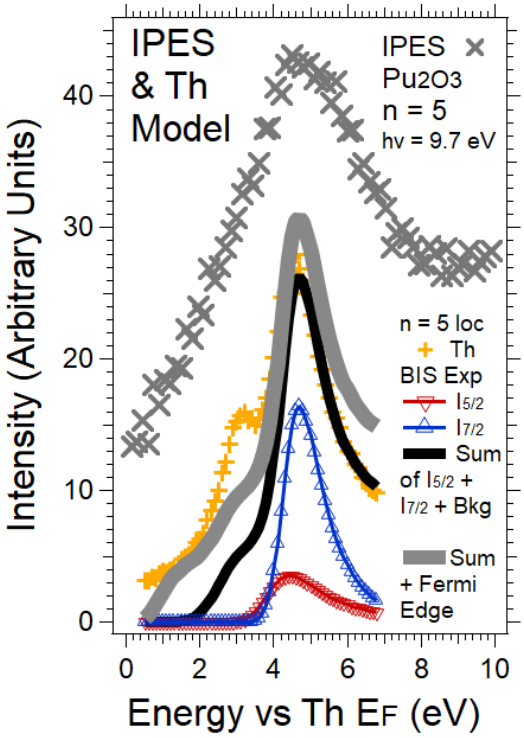

Figure 3 *A comparison between the IPES results for plutonium sesquioxide and the prediction of the Th Model for localized n = 5 is shown here. (Compare the grey line to the grey x.) The Fermi energy of the Pu_2O_3 was aligned with that for the Th BIS. The IPES spectrum was shifted vertically to facilitate comparison. Th Model: for the n = 5 localized case, ~4 electrons were added to the $5f_{5/2}$ manifold and ~1 electron was added to the $5f_{7/2}$ manifold, aiming for a 5/2 hole to 7/2 hole ratio of 0.29. This was done using a gaussian step cutoff with a FWHM of 1.0 eV, positioned horizontally producing a 5/2 hole to 7/2 hole ratio of 0.24 at an Energy of 7.0 eV. See text for details.*

The Underlying Simplicity of 5f Unoccupied Electronic Structure

The empirical model 5f UDOS is based upon the BIS measurement of elemental Th by Baer and Lang [12] and supported by calculations of the 5f DOS and related spectral results using FEFF. FEFF is a Green's Function based platform for spectral simulations [17-22], whose application to actinide 5f and related systems has been described elsewhere in detail. [23-28]. For now, the discussion will be limited to simple localized systems, paralleling the observation that the Intermediate Coupling Model has been found to work best with localized cases. By simple localized systems, it is meant that there is no further mixing of the $5f_{5/2}$ and $5f_{7/2}$ states by delocalization, magnetization or other perturbations. In this model, the Aufbau Principle [29,30] will be utilized, filling the 5f states sequentially from the bottom upwards. All of this will be described in detail below. The organization of the remainder of the paper is as follows: a section describing experimental and computational procedures; the fitting of the Th BIS spectrum; the FEFF results; the Aufbau procedure and generation of simulated spectra; and summary and conclusions.

II EXPERIMENTAL and COMPUTATIONAL

The HERFD experiments were performed using a Si(111) monochromator and a high-resolution Johansson-type spectrometer [16] operating in the tender x-ray regime (1.5 - 4.5 keV), on Beamline 6-2a at the Stanford Synchrotron Radiation Lightsource. The total energy resolution broadening of the HERFD experiment is about 0.8 eV. This produced a sharpening the U M_4/M_5 spectroscopic features almost an order of magnitude when compared to conventional x-ray absorption spectroscopy. Further detail concerning the HERFD experiments is available elsewhere [14].

The Underlying Simplicity of 5f Unoccupied Electronic Structure

The Inverse Photoelectron Spectroscopy measurement was performed in house at the Atomic Weapons Establishment (AWE) using a Geiger-Mueller photon detection system, centered at hv = 9.7 eV and with a bandpass of about 1.0 eV. These experiments are described more fully in another publication [15].

FEFF is a Green's Function spectral simulation program used in x-ray absorption spectroscopy and related techniques, including self-consistent real space multiple-scattering code for simultaneous calculations of x-ray-absorption spectra and electronic structure, particularly for Extended X-ray Absorption Fine Structure (EXAFS). [17-22] In general, FEFF has proven itself to be a powerful data analysis tool, but with some limitations when applied to 5f related transitions. [23-28] Here, a cluster composed of 79 Th atoms in an fcc lattice, with an interatomic distance of 3.6 Å, was used as an approximation for bulk Thorium. (See inset in Figure 4.) The calculation was driven to self-consistency, including the 5f states. (The 5f states were unfrozen and were part of the self-consistent variation.) This resulted in the DOS shown in Figure 4 for the central Th atom, with $n_s = 0.661$, $n_p = 0.257$, $n_d = 2.382$, $n_f = 0.677$ and $n_{total} = 3.999$, excluding 6 electrons for the 6p shallow core levels near 18 eV. The value of $n_{total} = 3.999$ is very close to expected value of 4. [13] However, the $n_f = 0.677$ value is too large, as will be discussed below. However, even now, it is clear that the Th 5f levels are almost completely unoccupied.

One final note before proceeding: the large value of $n_d = 2.382$ and the non-zero values of $n_s = 0.661$ and $n_p = 0.257$ are consistent with the participation of the 6d, 7s and 7p in actinide bonding, as seen in previous cluster calculations. For a 79 atom Pu cluster, the average configuration for the extended basis set was $5f^{5.33}$, $6d^{2.16}$, $7s^{0.38}$, $7p^{0.13}$ [31,32]

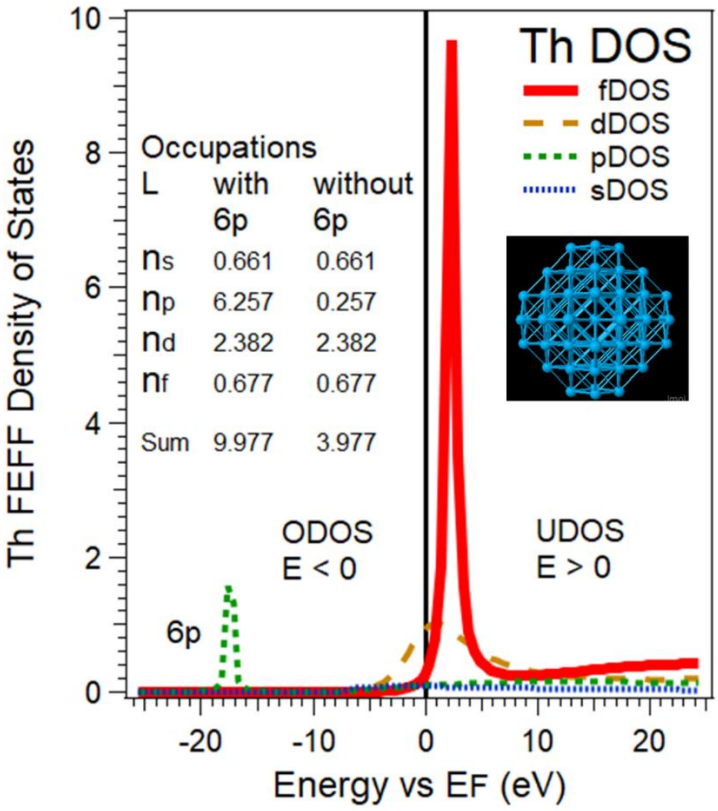

Figure 4

The L-specific FEFF DOS for the central atom of a 79-atom face-centered-cubic (fcc) cluster of Th. (See inset.) The occupied (unoccupied) DOS is a at energies below (above) the Fermi Level at zero eV. The p density near -18 eV is associated with the $6p_{1/2}$ and $6p_{3/2}$ levels and is assigned 6 electrons. The 5f levels were unfrozen. The L specific (s,p,d,f) occupations are also shown, with and without the 6p contribution.

III FEFF RESULTS and n_{5f} DETERMINATION

IIIa FEFF SPECTRAL SIMULATIONS

Before going on to the central issue of the determination of the 5f occupation in Th, it is of some utility to test the quality of the FEFF calculations. One way to calibrate the accuracy of FEFF calculations is via the comparison of spectral simulations with experimental data. To begin, consider the data shown in Figure 5. Here, the experimental results for the $N_{4,5}$ Electron Energy Loss (EELS) transitions [6] into the unoccupied 5f levels and the FEFF predictions for the $N_{4,5}$ XAS are plotted together. Because of the very high energy of the primary beam in the EELS experiment, this EELS and conventional XAS will be essentially identical [6,33]. As can

be easily seen in Figure 5, the experiment and simulation are in excellent agreement. Although FEFF calculations of XAS peak intensities and their corresponding Branching Ratios suffer from the absence of the proper inclusion of effects of 5f total angular momentum [25], that is not an issue here. Because the 5f levels are almost completely empty, the impact of neglecting the 5f total angular momentum coupling is nil. Hence, the very good agreement seen in Figure 5. Before moving on, it should be noted that the analysis in the original article [6] indicated that n_{5f} ~1/2. Assuming an error of ±0.01 in the BR value of 0.62 and applying the relationship in Equation 1 [9, 27], where the N's are the number of holes, with n + N = 14 and $n_{5/2} + N_{5/2} = 6$, then $n_{5f} = ½ \pm ¼$, from the BR analysis.

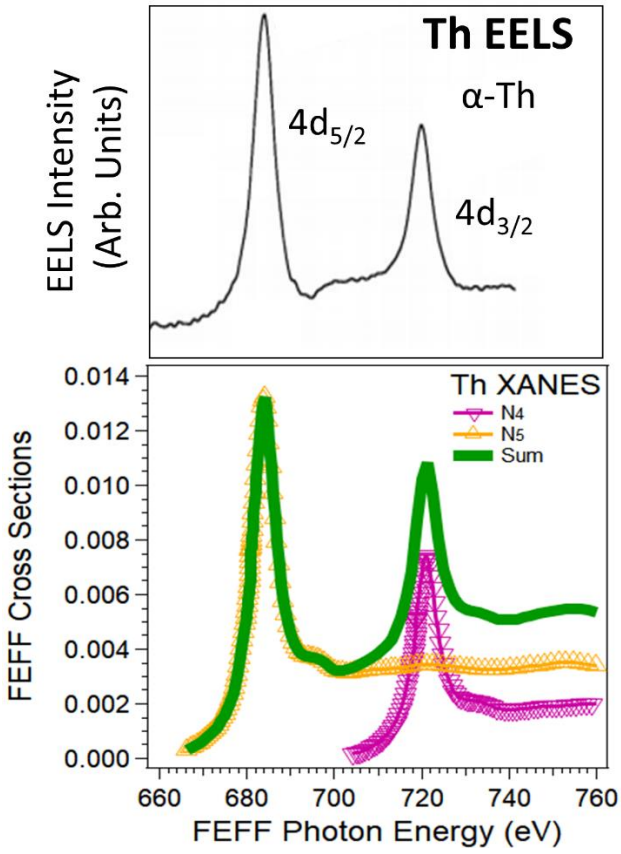

Figure 5
Shown here is a comparison of the $N_{4,5}$ EELS of alpha-Th and the XAS spectral simulation from the FEFF calculation. The EELS data were taken from [6,7]. The FEFF calculation was performed in absolute mode, to facilitate the proper scaling and addition of the N_4 and N_5 contributions. The EELS spectrum was shifted horizontally to align with the FEFF calculation peaks, but the energy differences match the FEFF energy scale.

The Underlying Simplicity of 5f Unoccupied Electronic Structure

$$BR = \frac{I_{\frac{5}{2}}}{I_{\frac{5}{2}} + I_{\frac{3}{2}}} = \left(\frac{1}{15}\right)\left(\frac{N_{5/2}}{N}\right) + \left(\frac{N_{7/2}}{N}\right) = 1 - \left(\frac{14}{15}\right)\left(\frac{N_{5/2}}{N}\right) \quad \text{Eq 1}$$

Another means to test the FEFF calculations and estimate the n_{5f} value is via the $O_{4,5}$ XES, shown in Figure 6. If the spectrum is Figure 6 is compared to the experimental results from Teterin et al. for $O_{4,5}$ XES for ThO_2 and ThF_4 [34, not shown here], substantial although incomplete agreement is found. Both sets of data have a large peak near 70 eV and a series of smaller features running to higher energies near 80 to 90 eV. It is reasonable to expect that both ThO_2 and ThF_4 would have low n_{5f} values, near zero, because of the 4+ oxidation state of the Th in these compounds. Thus, this agreement is further evidence of the validity of the FEFF calculations and the near zero value of n_{5f} in elemental Th.

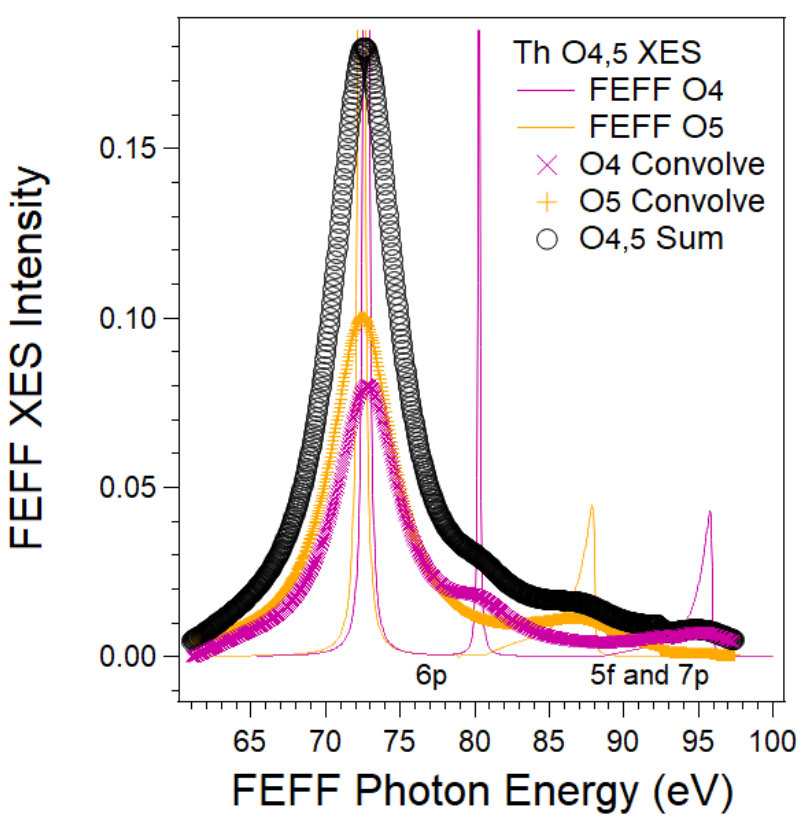

Figure 6
The $O_{4,5}$ XES of elemental Th, from the FEFF calculations, is shown here. A 5ev Full-Width-at-Half-Max (FWHM) Lorentzian has been convolved with the FEFF calculations. The convolved results are represented by the symbols x, +, and o. Note the presence of contributions from the $6p_{1/2}$, $6p_{3/2}$, 5f and 7p occupied states for both the O_4 and O_5 transitions. These assignments can be seen more clearly in Figure 7.

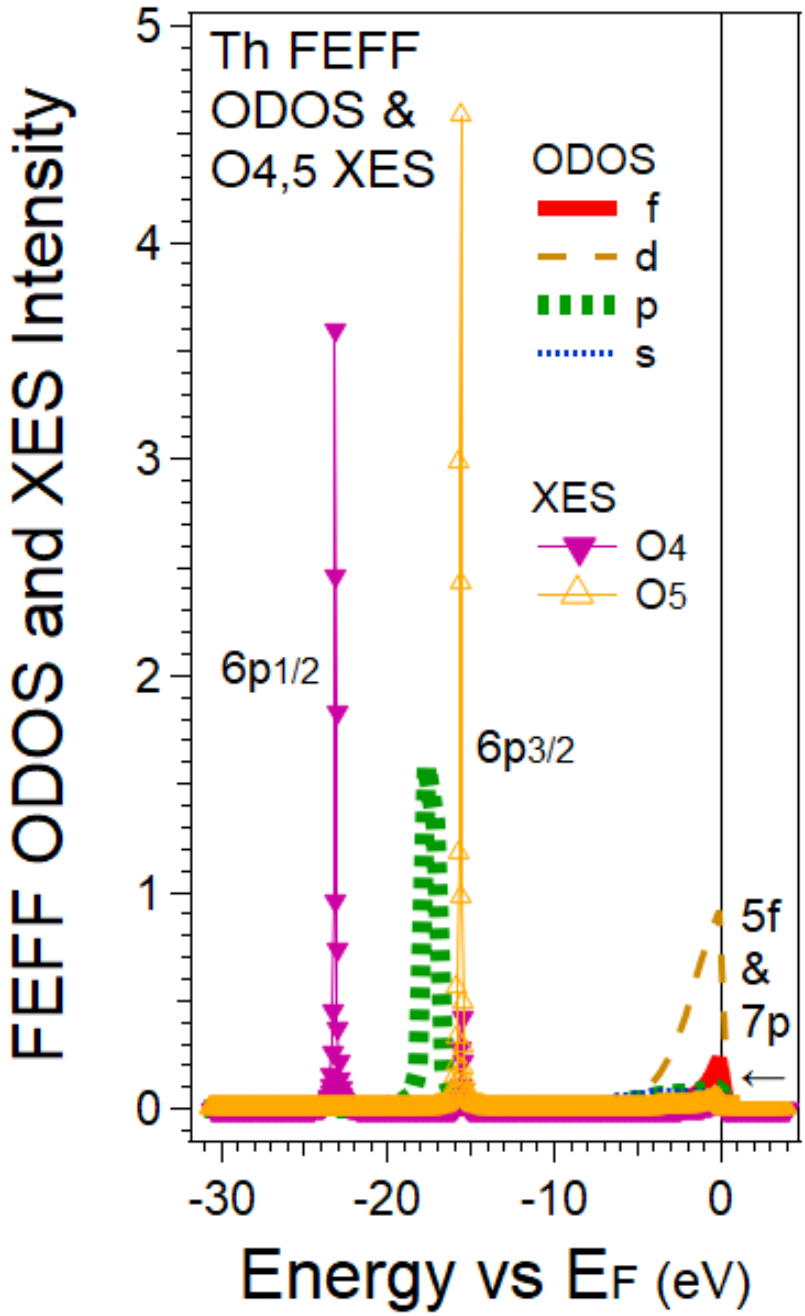

Figure 7
Comparison of $O_{4,5}$ spectra and ODOS. Illustrated here is a layover of the shifted O_4 and O_5 XES onto the ODOS, clearly showing the origin of the features in the combined spectrum in Figure 6. Note the small 5f feature near the Fermi Energy (E_F) at zero eV. There are strong electric dipole cross section effects in the $6p_{1/2}$ and $6p_{3/2}$ peaks. [23-25, 27] Transitions into the $O_{4,5}$ holes (empty d states) are only allowed from the 5f, 7p and 6p filled states. To align with the Fermi Energy onset, the XES spectra have been shifted as follows: for O_4, - 95.9 eV, for O_5, - 88 eV.

IIIb FEFF n_{5f} DETERMINATION

For the analysis that follows, it is critical to know the correct value of the 5f occupation, n_{5f}. At this point, it is of some utility to compare the FEFF L-specific DOS to the BIS

measurement of Baer and Lang. [12] (The BIS of Th has been shown to be in good agreement with the more sophisticated and j-specific Density of States calculations of Kutepov. [7, 9 - 11]) Here, the curves have been aligned on the Fermi Energy (E_F) at zero eV. The vertical scaling of the BIS spectrum is arbitrarily chosen to enhance the comparison. Note that the DOS at the Fermi Energy is composed primarily of 6d density, consistent with the Fermi step in the BIS spectrum, and that the 5f DOS are shifted upwards in energy. It is important that the BIS 5f DOS is shifted further than the FEFF 5f DOS. This strongly suggests that the initial 5f occupation estimate from the FEFF calculation is too high and needs to adjusted downward. This can be done by calculating the sum of the 5f FEFF density as a function of energy, as shown by the dot-dash orange curve, where the value has been multiplied by 10 to put it on the same scale as the other curves. At the Fermi Energy, the Sum*10 curve has a value near 7, as expected from 0.677*10. If the FEFF 5f DOS and the Sum*10 curve were each shifted to the right approximately 2 eV, then the FEFF 5f peak would align with the experimental BIS peak and the Sum*10 curve would have a value at the Fermi Energy of about 2, giving an adjusted n_{5f} value of 2/10 = 0.2.

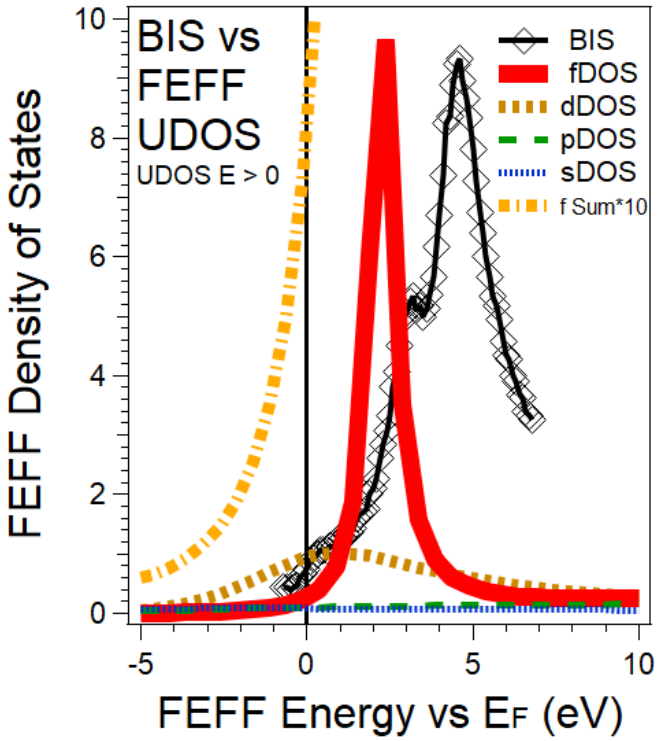

Figure 8
Presented here is a comparison of the FEFF DOS results and the experimental BIS result of Baer and Lang [12] See legend and text for details.

The estimates of the 5f occupation values are summarized in Table 1. This leads to the best estimate of the 5f occupation to be ¼ ± ¼. For the sake of simplicity and to be consistent with the historical perspective from the Naegele review [13], the value chosen for further use in the analysis below is $n_{f5} = 0$. At worst, this would leak to an error of (1/4)/14 = 0.018 = 1.8%, which is acceptable for the purposes herein.

Table 1: n_{5f} estimates and sources

n_{5f}	Description	Reference
0	$5f^0 (6d7s)^4$ Electron Configuration	13
x, small	$5f^x (6d7s7p)^{4-x}$ Electron Configuration	35
½ ± ¼	$N_{4,5}$ Branching Ratio	6
0.677	FEFF calculation-Initial	This paper
0.2	FEFF calculation-Adjusted	This paper
¼ ± ¼	Best Estimate	
0	Value utilized with error of ≤ 1.8%	

IV FITTING OF THE BIS SPECTRUM

From other measurements and analyses, there is much evidence to assert that the Bremstrahlung Isochromat Spectroscopy of the Actinides is dominated by the empty 5f states and that the BIS spectrum provides a good measure of the 5f UDOS. Consider the case of Uranium metal, α-U. It has been shown that the BIS spectrum agrees very well with the j-specific 5f density of state calculations of Kutepov. [7, 9, 10] It has also been demonstrated that the recent HERFD of Uranium Dioxide [14] can be summed to give a measure of the 5f UDOS that is again in very good agreement with earlier BIS measurements. [36] Finally, there is very good agreement between the calculated DOS of Th from Kutepov [7], again j specific with $5f_{5/2}$ and $5f_{7/2}$ manifolds, and the measured BIS of Th by Baer and Lang. [12] Hence, this analysis proceeds from the viewpoint that the BIS is representative of the 5f UDOS, and that the two

lobes in the Th BIS spectrum of Figure 8 are, in fact, the $5f_{5/2}$ and $5f_{7/2}$ components. If we then assume that the 5f states in Th are essentially completely empty, it is reasonable to assert that the relative intensity of the two lobes should be 6:8, for the $5f_{5/2}$ and $5f_{7/2}$ components, corresponding to the number of empty states. Remember, (1) that BIS has a significant amount of energy and angular averaging, (2) that the samples were polycrystalline, and (3) that the electronic transitions would involve d and p components of the incoming plane wave and the completely empty and spherically symmetric 5f spherical harmonics, thus tending to reduced cross section effects. All of these factors would tend to mitigate any possible cross section effects like those seen in XAS Branching Ratio measurements.

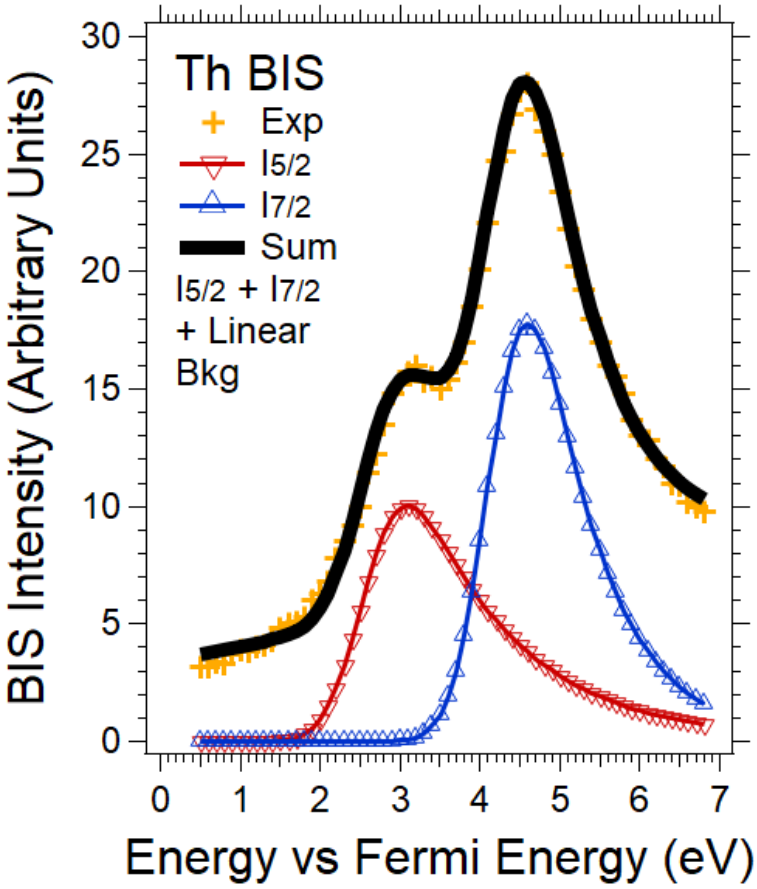

Figure 9
Shown here are the results of the fitting of the Th BIS experimental curve (orange +). The BIS data is from Baer and Lang [12]. Note the asymmetry of each of the peak functions. The background was linear. The $I_{5/2}$ ($I_{7/2}$) peak uses inverted red (upright blue) triangles. The sum of the $I_{5/2}$ peak, $I_{7/2}$ peak and linear background is presented as a thick black line.

Thus, the BIS experimental data was fitted with two peak functions and a linear background, in order to keep the analysis as simple as possible. The peak functions chosen were asymmetry gaussians, each generated by the convolution of a gaussian function with an exponential. An asymmetric function is needed, based upon the results of recent HERFD measurements. [14, 37-39] Except for one restriction, all fitting parameters were allowed to vary freely. The only restriction was that the gaussian widths in both functions were the same and that this value was constrained so that the relative integrated intensities of the first and second peak were of the ratio of 6:8, as described above. The gaussian width used was 0.389 eV. Again, the gaussian width is the width of the unperturbed gaussian function, before the application of the convolution with the exponential, that generates the asymmetry. The result of this operation is shown in Figure 9.

V AUFBAU PROCEDURE and GENERATION OF SIMULATED SPECTRA

To generate the simulated spectra, it is necessary to fill the 5f states from the bottom up, consistent with the Aufbau Principle [29,30] and the predictions of the Intermediate Coupling Model [6-8]. Effectively, this was done by applying a gaussian step function to the curves in Figure 9. The gaussian step function had a width of 1 eV. This would correspond to the (10% height-90% height) width of the step and the FWHM of the gaussian peak function. One great advantage of restricting the analysis here to simple localized systems is that the Intermediate Coupling Model can be used to predict the 5/2:7/2 ratio of number of holes for a given occupation, as well as the number of electrons in each manifold. [6,7] The number of holes and the ratio were again calculated by summing the peak intensities, as in Figure 9, but this time for

the truncated peaks. (Again, the truncated peaks are the result of the application of the gaussian step function to the two asymmetric peaks in Figure 9, the mathematical operation that simulates the Aufbau filling of the 5f states from the bottom upwards.) The results of these operations are shown in Table 2. As can be seen, for n = 2 and n = 3, there is very good agreement between the Aufbau generated peaks and the predictions of the Intermediate Coupling Model. For n =5, there is still agreement but not as good. This degradation as n increases is neither unexpected nor unreasonable. The error would naturally increase in the peak tails. Nevertheless, the model is still working, albeit less well, even at n = 5.

It is these truncated peaks that can be seen in Figures 1, 2 and 3. Note that in the HERFD figures, Fig. 1 and 2, there is excellent agreement between the measured M_4 and M_5 spectra and the Th model predicted curves in the lower section. In the HERFD experiment, the relative scaling of the M_4 and M_5 spectra was achieved by (1) matching the EXAFS and then (2) applying the BR intensity ratios to the EXAFS region of the M_4 and M_5 spectra, at slightly higher energies than those shown in Figures 1 and 2. (This process is explained in Reference [14].) In the HERFD experiment, the electric dipole selection rules should be strong and effective, based upon the extensive success of the Intermediate Coupling Model to explain the Branching Ratio results from conventional XAS. [9, 14, 27] These selection rules indicate that the M_4 spectrum should be only from the $5f_{5/2}$ UDOS and that the M_5 spectrum should be mainly, almost entirely, from the $5f_{7/2}$ UDOS. [14] This is also confirmed by the successful simulation of the HERFD peaks by the Th Model. Note also how the $5f_{7/2}$ UDOS remains essentially unchanged in going from n = 2 to n =3, but the major change is the reduction of the $5f_{5/2}$ UDOS as one hole is lost, again consistent with the experimental HERFD result. Finally, it is possible to sum the M_4 and

M_5 contributions (green line with filled circles) and compare it to the sum in the Th model (black line) and again there is excellent agreement, confirming the earlier comparison of UO_2 HERFD and BIS [14].

Table 2. A comparison of the number of electrons, holes, and their ratios, for the truncated peaks and from the Intermediate Coupling Model. [7]

Th Model		$5f_{5/2}$	$5f_{7/2}$	Ratio (5/2:7/2)	Int. Coupling Ratio (Holes)
n = 0 loc	Holes N	6	8	0.75	0.75
	Electrons n	0	0	0	
	Int Coupling Electrons n	0	0	0	
n = 2 loc	Holes N	3.95	7.94	0.50	0.51
(UF_4)	Electrons n	2.05	0.06		
	Int Coupling Electrons n	1.96	0.04		
n = 3 loc	Holes N	3.12	7.75	0.40	0.41
(UCd_{11})	Electrons n	2.88	0.25		
	Int Coupling Electrons n	2.79	0.21		
n = 5 loc	Holes N	2.0	6.8	0.29	0.24
(Pu_2O_3)	Electrons n	4.0	1.2		
	Int Coupling Electrons n	4.23	0.77		

Finally, there is again very good agreement between the measured Inverse Photoelectron Spectrum (IPES) at hv =9.7 eV and the prediction of the Th BIS model, as can be seen in Figure 3. This sample is composed of a Pu_2O_3 layer formed on top of a Pu substrate. [15] Based upon oxidation number arguments, Pu_2O_3 is an n= 5 material. It also has the advantage of relative surface stability over both Pu metal and PuO_2: Pu metal tends to oxidize quite readily and Pu_2O_3 has shown a propensity to form spontaneously on the surface of PuO_2. [40, 41], Because this measurement is IPES and not HERFD, other non-5f UDOS can contribute. Thus, the black

curve in Figure 3 shows an additional gaussian step cutoff, as an attempt to simulate the expected conduction band onset, from the 6d states (brown dash) in Figure 8. The height of the gaussian step has been chosen again to be unity and the width was 1 eV, consistent with the gaussian step used earlier. However, the placement along the energy axis was chosen arbitrarily. Additionally, it is likely that not only will Pu_2O_3 contribute to the spectrum, but also possibly there will be a weak signal from the Pu metal underneath. Because of that, an additional gaussian step has been added, for the expected Fermi Edge of the Pu substrate under the plutonium oxide layer. The placement of this step along the energy axis roughly corresponds to E_F but the choice of the relative magnitude was arbitrary. (The E_F in the Pu_2O_3 spectrum was aligned with the E_F from the Th.) This last curve is shown as a grey line.

Before moving on to the summary and conclusions, it is worthwhile to note that Vitova and coworkers have measured the M_5 HERFD of PuO_2^{2+} and the M_4 HERFD of UO_2^{2+} [39]. These are beautiful spectra of actinide ions in solution. Qualitatively, both of these spectra exhibit the same asymmetric tailing as in the spectra and model results in Figure 1, 2 and 3, with the caveat that the tails contain more pronounced peaking, probably from the actinyl bonding and in aquo solvation effects. Further comparison with the Th model beyond this discussion is hampered by the absence of the complementary peak for each: the M_4 HERFD of PuO_2^{2+} and the M_5 HERFD of UO_2^{2+}. Additionally, the effective 5f occupation for each is unclear. The plus two charge on each ion suggests that the U is n = 0 and the Pu is n = 3, but oxidation of the 5f levels is a matter of contention and the exact 5f occupation of each is uncertain.

VI SUMMARY and CONCLUSIONS

A simple empirical model based upon the Bremstrahlung Isochromat Spectroscopy (BIS) of elemental Th has been used to explain the recent High Energy Resolution Fluorescence Detection (HERFD) measurements of UF_4 (n =2) and UCd_{11} (n =3) as well as the new Inverse Photoelectron Spectroscopy (IPES) of Pu_2O_3 (n=5), where n is the 5f occupation number. Utilizing both experiment and theory, it was shown that Th 5f states are essentially empty, as a prelude to the further analysis and development of the model. This simple model provides a unified and consistent picture of 5f Unoccupied Density of States (UDOS), as the 5f occupation varies in the early part of the series for simple localized systems. Where, by simple localized systems, it is meant without delocalization, magnetic ordering or other sources of additional mixing between the j = 5/2 and j = 7/2 manifolds, beyond the constraints of the Intermediate Coupling Model.

ACKNOWLEDGEMENTS: Stanford Synchrotron Radiation Light-source is a national user facility operated by Stanford University on behalf of the DOE & OBES. LLNL is operated by Lawrence Livermore National Security, LLC, for the U.S. Department of Energy, National Nuclear Security Administration, under Contract DE-AC52-07NA27344.

DATA AVAILABILITY: The data that support the findings of this study are available from the corresponding author upon reasonable request.

References

1. S.S. Hecker, MRS Bull. **26**, 672 (2001).
2. S. J. Zinkle and G. S. Was, Acta Mater. **61**, 735 (2013).

3. Nuclear Energy Institute, Nuclear shares of electricity generation, http://www.world-nuclear.org/info/nshare.html
4. I. L. Pegg, Phys. Today **68**, 33 (2015).
5. K.T. Moore, et al., Phys. Rev. Lett. **90**, 196404 (2003).
6. G. van der Laan, et al., Phys. Rev. Lett. **93**, 097401 (2004).
7. J.G. Tobin, et al.,Phys. Rev. B **72**, 085109 (2005).
8. G. van der Laan and B. T. Thole, Phys. Rev. B **53**, 14458 (1996).
9. J. G. Tobin, S. Nowak, S.-W. Yu, R. Alonso-Mori, T. Kroll, D. Nordlung, T.-C. Weng, D. Sokaras, Applied Sciences **10**, 2918 (2020), http://www.mdpi.com/2076-3417/10/8/2918, Erratum https://www.mdpi.com/2076-3417/10/12/4242.
10. J. G. Tobin, S.-W. Yu, and B.W. Chung, Top. Catal. **56**, 1104(2013).
11. J.G. Tobin, J. Electron Spectroscopy and Rel. Phen. **194**, 14 (2014).
12. Y. Baer and J.K. Lang, Phys Rev B **21**, 2060 (1980).
13. J.R. Naegele, "Actinides and Some of their Alloys and Compounds," Electronic Structure of Solids: Photoemission Spectra and Related Data, Landolt-Bornstein "Numerical Data and Functional Rel. in Sci. and Tech.," ed. A Goldmann, Group III, Volume **23b**, Pages 183 – 327 (1994); and ref. therein.
14. J. G. Tobin, S. Nowak, C.H. Booth, E.D. Bauer, S.-W. Yu, R. Alonso-Mori, T. Kroll, D. Nordlung, T.-C. Weng, D. Sokaras, J. El. Spect. Rel. Phen. **232**, 100 (2019).
15. P. Roussel, J. Electron Spectroscopy Rel. Phen. **246** 147030 (2021).
16. S. H. Nowak, C. Schwartz, R. Armenta, A. Gallo, D. Day, S. Christensen, R. Alonso-Mori, T. Kroll, D. Nordlund, T.-C. Weng, and D. Sokaras, Rev. Sci. Instrum. **91**, 033101 (2020).
17. A. L. Ankudinov, A. I. Nesvizhskii, and J. J. Rehr Phys. Rev. B **67**, 115120 (2003).
18. J.J. Rehr, J.J. Kas, F.D. Vila, M.P. Prange, K. Jorissen, Phys. Chem. Chem. Phys. **12**, 5503-5513 (2010).
19. J.J. Rehr, J.J. Kas, M.P. Prange, A.P. Sorini, Y. Takimoto, F.D. Vila, Comptes Rendus Physique **10** (6) 548-559 (2009).
20. J. J. Rehr and R. C. Albers, Rev. Mod. Phys. **72**, 621, (2000).
21. A. L. Ankudinov, A. I. Nesvizhskii, and J. J. Rehr, Phys. Rev. B **67**, 115120 (2003).
22. A. L. Ankudinov, S. D. Conradson, J. Mustre de Leon and J. J. Rehr, Phys. Rev. B **57**, 7518 (1998).
23. J. G. Tobin, S.-W. Yu, and D. Sokaras, J. El. Spect. Rel. Phen. **246**, 147007 (2021).
24. J. G. Tobin and D. Sokaras, MRS Advances **5**, 2631 (2020).
25. J. G. Tobin and D. Sokaras, J. Vac. Sci. Tech. A **38**, 036001 (2020).
26. J. G. Tobin, S. Nowak, S.-W. Yu, R. Alonso-Mori, T. Kroll, D. Nordlung, T.-C. Weng, D. Sokaras, Surface Science **698**, 121607 (2020).

27. J. G. Tobin, S. Nowak, S.-W. Yu, R. Alonso-Mori, T. Kroll, D. Nordlung, T.-C. Weng, D. Sokaras, J. Phys. Commun. **4**, 015013(2020).
28. J. G. Tobin, S.-W. Yu, D.K. Shuh and D. Sokaras, J. Phys. Soc. of Japan **89**, 024711 (2020).
29. C. Kittel, "Introduction to Solid State Physics," John Wiley and Sons, New York, 1976.
30. https://en.wikipedia.org/wiki/Aufbau_principle
31. M.V. Ryzhkov, A. Mirmelstein, S.-W.Yu,B. Chung and J.G. Tobin, lnt. J. Quantum Chem. **113**, 1957 (2013).
32. M.V. Ryzhkov, A. Mirmelstein, B. Delley, S.-W. Yu, B. Chung and J.G. Tobin, J. Electron Spectroscopy and Rel. Phen. **194**, 45 (2014).
33. K. T. Moore, B. W. Chung, S. A. Morton, A. J. Schwartz, J. G. Tobin, S. Lazar, F. D. Tichelaar, H. W. Zandbergen, P. Soderlind and G. van der Laan, Phys. Rev. B **69**, 193104 (2004).
34. Yu.A. Teterin, V.A. Terekhov, A.Yu. Teterin, K.E. Ivanov, I.O. Utkin, A.M. Lebedev, L. Vukchevich, J. Electron Spectroscopy Rel. Phen. **96**, 229–236 (1998).
35. J.G. Tobin, MRS Advances **3** (53), 3149 – 3154, (2018).
36. Y. Baer and J. Schoenes, Solid State Commun. **33**, 885 (1980).
37. K.O. Kvashnina, S.M. Butorin, P. Martin, P. Glatzel, Phys. Rev. Lett. **111**, 253002 (2013).
38. K. O. Kvashnina, H. C. Walker, N. Magnani, G. H. Lander, and R. Caciuffo, Phys. Rev. B **95**, 245103 (2017).
39. T. Vitova, I. Pidchenko, D. Fellhauer, P.S. Bagus, Y. Joly, T. Pruessmann, S. Bahl, E. Gonzalez-Robles, J. Rothe, M. Altmaier, M.A. Denecke and H. Geckeis, Nat. Comm. **8**, 16053 (2016).
40. M.T.Butterfield, T.Durakiewicz, E.Guziewicz, J.J.Joyce, A.J.Arko, K.S.Graham, D.P.Moore, L.A.Morales, Surface Science **571**, 74-82 (2004).
41. H.G. García Flores, P. Roussel, D. Moore, D.L. Pugmire, Surface Science **605** (3), 314-320 (2011).